THE ASTROPHYSICAL JOURNAL, 416:L45–L48, 1993 October 20

DARK MATTER HALOS IN ELLIPTICAL GALAXIES

FRANCESCO BERTOLA,[1] ALESSANDRO PIZZELLA,[2] MASSIMO PERSIC,[3,4] AND PAOLO SALUCCI[3]

Received 1993 June 1; accepted 1993 August 6

ABSTRACT

Values of the M/L_B ratio in the inner regions of elliptical (E) galaxies are determined using ionized gas disks as tracers of the triaxial potential. These data, when combined with those provided by the H I disks extending to the outer regions, show that the variation of M/L_B with galactocentric radius in Es is similar to that of spirals. In particular, it is found that in spirals and Es of the same visible mass the radius where the density of the dark matter equals that of the visible matter occurs at the same distance in units of r_e, namely at $1.2r_e$. This suggests a similar picture of baryonic collapse into a preexisting DM halo for both Es and spirals.

Subject headings: dark matter — galaxies: elliptical and lenticular, cD — galaxies: formation — galaxies: fundamental parameters — galaxies: kinematics and dynamics — galaxies: structure

1. INTRODUCTION

Recent attempts in modeling extended velocity dispersion profiles up to $1–2r_e$ in a sample of Es (Saglia et al. 1993) indicates no compelling evidence of dark matter (DM) out to $1–2r_e$. Consequently the presence of DM can be established only probing the potential further out using H I disks or X-ray envelopes. However, even using these tracers, the issue is still unsettled (Fabbiano 1989; Kent 1990; de Zeeuw 1992; Ashman 1992).

In this *Letter* we show that determinations of M/L based on studies of a single dynamical component, namely the gaseous disk (actually, the ionized gas disk and the H I disk for the inner and outer regions respectively) lead to a framework in which a parallel behavior in the M/L ratio versus radius can be defined both for spirals and Es.

2. ANALYSIS OF THE OBSERVATIONAL DATA

The analysis carried out in this *Letter* is based on data for eight Es possessing inner gaseous disks which, in four cases, are observed to extend to the outer regions. The velocity field, as derived from the emission lines of the ionized gas and from the 21 cm line of H I, provides information on the inner and outer mass distribution respectively. The galaxies are listed in Table 1 where the photometric data r_e and B_T^0 are reported together with the adopted distance ($H_0 = 50$ km s^{-1} Mpc^{-1}) and the corresponding luminosity.

For four galaxies of the sample, namely NGC 1052, NGC 4278, NGC 5266, and NGC 7097, we have derived the mass distribution in the inner region, taking into account that the gaseous disks are generally moving under the influence of a triaxial potential. A similar analysis has been carried out for NGC 5077 (Bertola et al. 1991). In a nonrotating triaxial galaxy, the gas orbits in one of the two allowed principal planes, perpendicular either to the longest axis (Y-Z plane) of the triaxial figure or to the shortest axis (X-Y plane). The orbits of the gas clouds are circular only in the outer regions, but they become increasingly elliptical toward the center (de Zeeuw & Franx 1989). In order to perform the analysis of the velocity field of the gas, it is necessary to determine the intrinsic shape of the host E galaxy and its orientation in space. To constrain the viewing angles θ (= inclination of the X-Y plane) and ϕ (= the azimuth of the Y-axis with respect to the line of nodes) and the possible axial ratios b/a, c/a, we used the following geometrical observations: the difference between the position angles of the stellar component's major axis, derived from isophotal mapping, and of the gaseous disk's major axis, derived from the analysis of the velocity field and from the Hα image; the ellipticity (ϵ_s) of the stellar component; the ellipticity (ϵ_g) of the ionized gas disk. Once the most representative values of b/a, c/a, θ, ϕ are selected, a best fit to the observed velocity field is made using a Stäckel-like potential to derive the density distribution. This procedure is carried out twice, on the assumption that the gas is settled on either the X-Y or the Y-Z plane. In the case that the geometrical constraints do not rule out one of the two planes, then the fit which gives the lower rms deviation from the observed velocity field is adopted. Velocity curves derived using a spherical potential fit equally well the observations, due to the lack of high-accuracy velocity measurements. We used velocity data from the following sources: Davies & Illingworth (1986) and Pizzella (1989) for NGC 1052; Demoulin-Ulrich, Butcher, & Boksenberg (1984) for NGC 4278; Varnas et al. (1987) and Caldwell (1984) for NGC 5266; Caldwell, Kirshner, & Richstone (1986) for NGC 7097. The photometric sources are listed in Table 1. The geometrical constraints used are listed in Table 2 together with the assumed values for b/a, c/a, θ, ϕ and the inclination of the gaseous disk's orbital plane, while the density distribution along the major axis and the trend of M/L_B are shown in Figure 1. The remaining data, used to derived the M/L_B distribution in Figure 2, are taken from the literature.

Figure 1 confirms the result already found for NGC 5077: the values of M/L_B based on a triaxial potential are substantially constant in the region considered. This justifies a representation of M/L_B constant out to $\sim r_e$ (see Fig. 2). On the other hand, the M/L_B ratios based on a spherical potential, in spite of showing larger variations with radius, have average values not appreciably different from those obtained with triaxial models. We now discuss our sample objects individually.

NGC 1052.—The major axis of the inner Hα disk (Kim 1989) is roughly aligned with the stellar minor axis. Available radial

[1] Dipartimento di Astronomia, Vicola dell'Osservatorio 5, I-35122, Università di Padova, Italy.
[2] Istituto Astronomico, Università di Roma, via Lancisi 29, Roma, Italy.
[3] SISSA, Strada Costiera 11, I-34014 Trieste, Italy.
[4] Osservatorio Astronomico, via G.B. Tiepolo 11, I-34131 Trieste, Italy.

TABLE 1

ELLIPTICAL GALAXIES WITH GASEOUS DISK

Object	Type	Distance (Mpc)	r_e	L_B^T (10^{10} $L_{B\odot}$)	$M/L(r)_{inner}$ [$M_\odot/L_{B\odot}(r_e)$]	$M/L(r)_{outer}$ [$M_\odot/L_{B\odot}(r_e)$]
NGC 1052	E4	28.2	34″[a]	3.62	2.5 (0.9)	8.7 (7.3)
NGC 2974	E4	38.5	34[b]	4.32	4.0 (0.9)	15.6 (3.3)
NGC 4278	E1–2	16.4	34[c]	1.72	4.0 (0.5)	45 (10)
NGC 5077	E3–4	56	19[d]	6.37	4.1 (1.3)	...
NGC 5128	S0pec	5[e]	305[e]	7.5[e]	3.1 (1.2)	...
NGC 5266	SA$^-$:	57.6	65[f]	13.5	3.0 (0.3)	...
NGC 7097	E5	52	19.3[g]	3.94	5.0 (0.9)	...
IC 2006	E	26	23[h]	1.27	...	16.3 (6.5)

NOTES.—Morphological type and L_B^T from RC3; distances are based on $H_0 = 50$ km s^{-1} Mpc^{-1}; next to the cumulative M/L_B's for the inner and outer region (in units of $M_\odot/L_{B\odot}$), the respective last measured points (in units of r_e) are indicated.

[a] Davies & Illingworth 1986.
[b] Djorgovsky 1985.
[c] Peletier et al. 1990.
[d] Bertola et al. 1991.
[e] van Gorkom et al. 1990.
[f] Varnas et al. 1987.
[g] Caldwell et al. 1986.
[h] Schweizer et al. 1989.

velocity measurements have been used out to a distance of 30″ ($\sim r_e$). The outer velocity measurements by Davies & Illingworth (1986) refer to the strongly warped SW side and hence are not used. Considering that the Hα disk is seen at an angle of 37°, the corresponding M/L_B curve turns out quite constant at $M/L_B = 2.5$, a value which is rather low if compared with $M/L_B = 10.5$ derived by Davies & Illingworth (1986) using stellar dynamics. On the NE side of NGC 1052, a 21 cm rotation curve is measured (van Gorkom et al. 1986) which remains flat at 200 km s^{-1} from 1′.4 to 4′ ($7.3r_e$). This outer disk, as seen at 21 cm, appears almost edge-on. Therefore, the gaseous disk is warped. The cumulative M/L_B out to $7.3r_e$, scaled to our adopted distance and luminosity, is $M/L_B = 8.7$.

NGC 2974.—From the kinematics of the gaseous disk (Amico et al. 1993; triaxiality is taken into account), $M/L_B \sim 3$ for $r \lesssim r_e$. The outer H I disk (Kim et al. 1988) has the same spatial orientation and extends out to 2′ ($3.2r_e$), rotating at 355 km s^{-1}. The M/L_B ratio within this distance, once rescaled to our distance and luminosity, is $M/L_B = 15.6$.

NGC 4278.—The kinematics of the inner Hα disk, extending out to $0.5r_e$, indicates a constant value of $M/L_B = 4$. For the H I disk (see Lees 1992), an outward increase of M/L_B, which nicely matches our value in the inner region, is found using a triaxial model. Our model parameters are fully consistent with those of Lees. In Figure 2 only the last point by Lees is plotted, scaled to our distance and total B-luminosity (assuming $B - R = 1.6$; Peletier et al. 1990).

NGC 5077.—This galaxy and its gaseous disk have been studied extensively by Bertola et al. (1991). We adopt $M/L_B = 4$ in the inner region.

NGC 5128.—Similar values of $M/L_B \sim 3$ are obtained from the 21 cm rotation curve of the gaseous disk (extending to $1.2r_e$) and from the mass distribution derived by Bland (1985) from the study of the ionized gas.

NGC 5266.—The analysis of the photometric data and of the velocity field of the ionized gas disk up to $0.3r_e$ shows that NGC 5266, an E4 elliptical, is an oblate galaxy (see also Vernas et al. 1987) with constant $M/L_B = 3$. This galaxy has been detected at 21 cm, but no rotation curve is available. From the width of this line, one can argue that the velocity continues to rise beyond the limit of the velocity data for the ionized gas.

NGC 7097.—Our fit to the velocity field (Caldwell et al. 1986) of this galaxy with a triaxial model gives a constant $M/L_B = 5$ up to $\sim 0.9r_e$.

IC 2006.—From the H I ring kinematics Schweizer, van Gorkom, & Seitzer (1989) derive $M/L_B = 16$ within $6.5r_e$. The inner $H\alpha$ disk, which extends to $\sim 1.5r_e$, shows a very low rotation velocity leading to unreasonably low values of M/L_B. However, assuming a different inclination of the inner disk, as in the case of a warped structure, could lead to more comfortable M/L_B values. In view of these considerations, we decided not to use the inner velocity data.

The data concerning the M/L_B are reported in Table 1 and plotted in Figure 2. The mean value of M/L_B out to $\sim r_e$, for

TABLE 2

TRIAXIAL MODELS: PARAMETERS

NGC (1)	Plane[a] (2)	b/a[b] (3)	c/a[b] (4)	θ[c] (5)	ϕ[c] (6)	i[d] (7)	PA$_s$[e] (8)	ϵ_s[e] (9)	PA$_g$[e] (10)	ϵ_g[e] (11)
1052.....	Y-Z	0.95	0.66	70°	50°	53°	113°[f]	0.28[f]	35°	0.5 ± 0.1[g]
4278.....	X-Y	0.85	0.83	57	−30	57	20[h]	0.05[i]	45	0.50 ± 0.05[h]
5266.....	Y-Z	1.00	0.60	73	65	66	110[j]	0.38[j]	27	0.65 ± 0.05[j]
7097.....	X-Y	0.80	0.30	63	10	63	18[k]	0.40[i]	14	0.45 ± 0.1[l]

[a] Orbital plane of the ionized gas.
[b] Axial ratios of the best fit.
[c] Viewing angles of the best fit (θ = inclination angle of the X-Y plane; ϕ = azimuthal angle in the X-Y plane of the Y-axis counted from the line of nodes.
[d] The inclination of the gaseous disk ($i = 90°$ for an edge-on disk).
[e] Geometrical constraints.
[f] Jedrejewski et al. 1987.
[g] Sparks et al. 1985.
[h] Demoulin-Ulrich et al. 1984.
[i] RC2.
[j] Varnas et al. 1987.
[k] Caldwell et al. 1986.
[l] Buson et al. 1993.

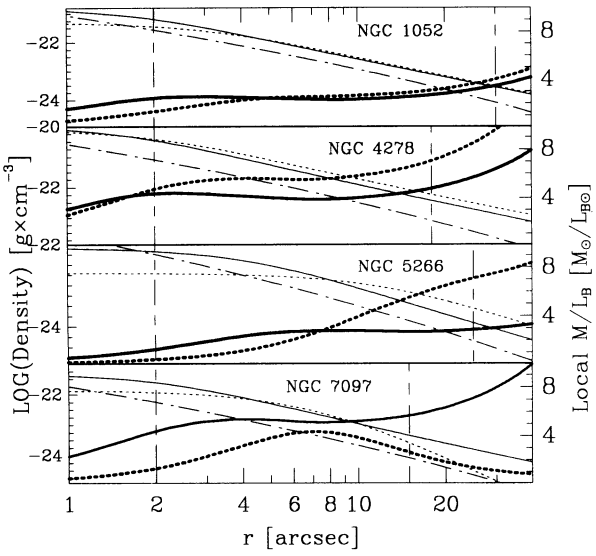

FIG. 1.—Mass density profile as a function of radius along the major axis: *solid line* = triaxial fit; *dotted line* = spherical fit. Light density profile: *dotted-dashed line*. Local M/L_B as a function of radius: *bold solid line* = triaxial; *bold dotted line* = spherical.

our sample of average luminosity $(1.2 \pm 0.3)L_B^*$, is 3.5 ± 0.9 [where $\log (L_B^*/L_{B\odot}) = 10.63$]. This value is in good agreement with that determined by van der Marel (1991), using stellar kinematics, for Es of about the same luminosity. This agreement is an a posteriori check of the proper use of the gaseous disk as mass tracer. Beyond r_e, the M/L_B ratios show a tendency to increase, with slopes that differ by at most a factor of 2.

3. MASS DISTRIBUTION IN ELLIPTICALS VERSUS SPIRALS

The data presented in the previous sections imply the existence, between r_e and $10r_e$, of progressively more substantial contributions of a non-luminous component to the gravitating matter, similar to what is observed in spirals.

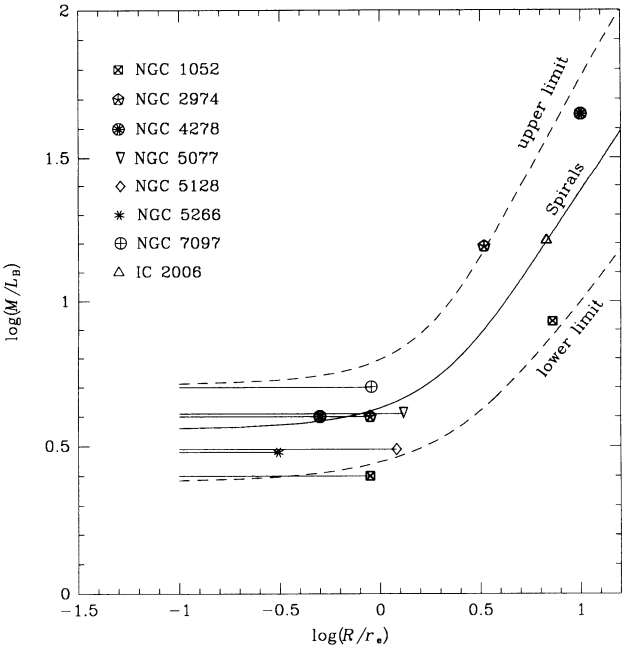

FIG. 2.—Cumulative M/L_B as a function of radius for L_B^* spiral galaxies plotted over the ellipticals' data (*solid line*). The dashed lines represent the uncertainties associated with the mass decomposition in eq. (1).

Two major components describe the mass structure of normal spirals: (1) a thin exponential disk with surface-density distribution $I(r) = I_0\, e^{-r/R_D}$ (with R_D the disk length scale; note that $r_e = 1.68R_D$); and (2) a spherical pseudoisothermal dark halo with density distribution $\rho(r) = \rho_0/[1 + (r/a)^2]$ [where the core radius $a = (1.4 \pm 0.5)r_e$; see Salucci & Frenk 1989]. Using these two mass components alongside the scaling relations for their basic parameters (Persic & Salucci 1990, 1991; Salucci & Frenk 1989), we can write the average M/L_B curve for an L_B^* spiral as

$$\frac{M}{L_B} \simeq 1.2^{+0.3}_{-0.3} + \frac{3.7^{+10.3}_{-2.8}}{1 - (1 + 1.68r/r_e)e^{-1.68r/r_e}} \times \left(\frac{r}{1.4^{+0.5}_{-0.5}\, r_e} - \tan^{-1} \frac{r}{1.4^{+0.5}_{-0.5}\, r_e} \right), \quad (1)$$

where the first and second term on the right-hand side refer to the luminous and the dark component, respectively. (The quoted uncertainties reflect observational errors and errors intrinsic to the mass decomposition method; see Persic & Salucci 1990.) Since the luminous mass converges rapidly (85% of the mass of an exponential disk is contained within $2r_e$) and the halo mass keeps growing (at small radii like r^3 and then like r), then the inner ($r \lesssim r_e$) and outer ($r \gg r_e$) regions are respectively luminous- and dark matter–dominated, while at intermediate radii ($r \simeq 2r_e$) both components contribute to the dynamics.

The M/L_B curve for L_B^* spirals, plotted (together with the curves expressing the uncertainties; see eq. [1]) in Figure 2 as a function of r/r_e, matches nicely the data for L_B^* ellipticals (of course the luminous M/L_B has been shifted upward to account for the higher zero-point of the elliptical galaxies' M/L_B). The effect of replacing the exponential profile with a de Vaucouleurs profile in the light distribution is negligible. It should be noted that r_e is about 2 times larger for spirals than for Es of comparable luminosity (Kent 1985, 1990). Nevertheless, the normalized radius r/r_e turns out to be a natural "homology coordinate" for the M/L_B distribution of spirals and Es.

Having preliminarily established some similarity in the M/L_B structure of spirals and Es, we now attempt to derive some DM properties of Es from a direct modeling of the observed mass-to-light curves by means of a theoretical model. Unfortunately, the limited statistics of our data (18 independent points) will allow testing a model of only a limited number of free parameters. We will look, in particular, for a luminosity dependence of the DM content of Es, similar to what has been done for spirals (Persic & Salucci 1990; Ashman, Salucci, & Persic 1993): the small range in luminosity spanned by our sample, however, will make any such results somewhat preliminary. In detail, our model consists of a luminous de Vaucouleurs spheroid with $M/L_B = 3.5$ plus a spherical halo with

$$M_{\rm halo}(r) = M^*_{\rm halo}(r_3)\left(\frac{L_B}{L_B^*}\right)^{\gamma} \frac{(r/a) - \tan^{-1}(r/a)}{(r_e/a) - \tan^{-1}(r_e/a)}\,.$$

The best-fit solution of this model against the data is

$$M^*_{\rm halo}(r_e) = (1.3 \pm 0.4) \times 10^{10}\, M_\odot\ ;$$
$$\gamma = 0.3 \pm 0.1\ ;\quad a = 1.2^{+0.3}_{-0.2}\, r_e\,. \quad (2)$$

Pending confirmation, we point out two remarkable regularities between the halos of spirals and Es. For both types of object, the core radius, even though different in physical units,

is $\sim 1.3r_e$. Then, simple calculations show that spirals (see also Ashman et al. 1993) and Es of the same visible mass have comparable halo masses at r_e, roughly $10^{10}[M_{\rm lum}/(5 \times 10^{10}\ M_\odot)]^{0.3}\ M_\odot$. It should be emphasized, however, that while scaling laws of DM properties with luminosity are known for spirals (Persic & Salucci 1990; Broeils 1992; Ashman 1993), in the case of Es, the investigation of this issue will require studying a sample spanning a larger range in luminosity. If the analogy with spirals can be extended any further, i.e., if the scaling properties with luminosity of the dark and visible components deduced for spirals can be expected to hold also for Es, then we would expect that for increasing luminosity M/L_B should show a tendency to increase at a fixed $r/r_e < 1$ (see van der Marel 1991) and to decrease at a fixed $r/r_e > 1$. Indeed, even though it may still be a coincidence, this qualitative trend is implied by our preliminary result in equation (2).

In Figure 3 we plot the visible and dark matter densities of Es and spirals with the same visible mass (we take for reference the mass of an L_B^* elliptical, $M_* = 1.5 \times 10^{11}\ M_\odot$). These correspond, for the Es and the spirals respectively, to a deprojected de Vaucouleurs profile with $r_e = 5$ kpc and a pseudoisothermal halo with $a = 6$ kpc, and to a spherical effective distributtion of a Freeman disk with $R_D = 8.5$ kpc and a halo with $a = 20$ kpc.

From Figure 3 it is clear that Es are more concentrated than spirals in *both* their visible and dark components. Remarkably, in both systems the radius $R_{\rm cross}$, defined as the radius where $\rho_{\rm DM} = \rho_{\rm VM}$, is $R_{\rm cross} = 1.2r_e$. Thus the half-light radius turns out as the radius that determines the scale where the DM starts dominating the mass distribution. We emphasize that this interrelation between the distributions of the dark and the luminous matter has to be accounted for by any theory of galaxy formation. In view of the above results, we propose that Es and spirals (at the same visible mass) may be viewed as *different stages* of the collapse of a gaseous protocloud into a preexisting DM halo. For an M_* spiral the collapse is halted at $R^S_{\rm cross} = 17$ kpc by the angular momentum likely acquired at turnaround. Conversely, in the case of a M_* elliptical the original angular momentum of the baryon component has been dissipated during the violent relaxation process, and the collapse has proceeded down to $R^E_{\rm cross} = 6$ kpc where it has been halted by the pressure of the violently relaxed stellar component. In this scenario the Es and spirals of same visible mass were originally embedded in similar halos. The extra collapse experienced by the visible matter in Es with respect to

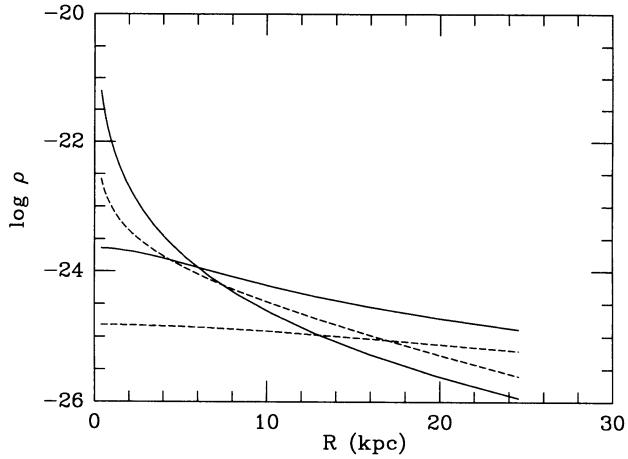

FIG. 3.—The radial behaviors of the luminous and dark matter profiles for an elliptical (*solid lines*) and a spiral (*dashed lines*) of the same visible mass $M_{\rm lum} = 1.5 \times 10^{11}\ M_\odot$. In both cases, the luminous and the dark matter densities intersect at $1.2r_e$, which roughly corresponds to the respective halo core radii.

spirals has produced an extra-compression in the original DM halo. To look at this, from the curves in Figure 3 (and considering also Ashman et al. 1983) we compute, for a M_* elliptical and a M_* spiral, the quantities $\delta M_{\rm VM}/M_{\rm VM} \equiv [M^{\rm E}_{\rm VM}(6\ {\rm kpc}) - M^{\rm S}_{\rm VM}(6\ {\rm kpc})]/M^{\rm S}_{\rm VM}(17\ {\rm kpc})$ which is a measure of the amount of the further collapse of the visible matter in Es and $\delta M_{\rm DM}/M_{\rm DM} \equiv [M^{\rm E}_{\rm DM}(6\ {\rm kpc}) - M^{\rm S}_{\rm DM}(6\ {\rm kpc})]/M^{\rm S}_{\rm DM}(17\ {\rm kpc})$ which represents the resulting compression of the DM. We find $\delta M_{\rm VM}/M_{\rm VM} \sim \delta M_{\rm DM}/M_{\rm DM} \sim 0.5$, thus supporting the above proposed scenario.

4. CONCLUSIONS

From the above results, a tentative unified mass structure scheme has emerged for spiral and E galaxies, the effective radius, r_e, being in both cases the "homology coordinate" for the M/L_B distribution. Gaseous disks have proven to be powerful tools in this kind of analysis. The collection of more data, especially at 21 cm, will allow us to better define (notably as a function of luminosity) the properties of DM in Es.

We are grateful to Tim de Zeeuw and Dave Burstein for useful comments on the manuscript.

REFERENCES

Amico, P., et al. 1993, in Structure, Dynamics and Chemical Evolution of Elliptical Galaxies, ed. I. J. Danziger, W. W. Zeilinger, & K. Kjär (ESO/EIPC Workshop), 225
Ashman, K. M. 1992, PASP, 104, 1109
Ashman, K. M., Salucci, P., & Persic, M. 1993, MNRAS, 260, 610
Bertola, F., Bettoni, D., Danziger, I. J., Sadler, E. M., Sparke, L. S., & de Zeeuw, P. T. 1991, ApJ, 373, 369
Bland, J. 1985, Ph.D. thesis, Univ. of Sussex
Broeils, A. H. 1992, Ph.D. thesis, Gronigen Univ.
Buson, L. M., et al. 1993, in preparation
Caldwell, N. 1984, ApJ, 278, 96
Caldwell, N., Kirshner, R. P., & Richstone, D. O. 1986, ApJ, 305, 136
Davies, R. L., & Illingworth, G. D. 1986, ApJ, 302, 234
Demoulin-Ulrich, M.-H., Butcher, H. R., & Boksenberg, A. 1984, ApJ, 285, 527
de Zeeuw, P. T. 1992, in Morphological and Physical Classification of Galaxies, ed. G. Longo, M. Capaccioli, & G. Busarello (Dordrecht: Kluwer), 139
de Zeeuw, P. T., & Franx, M. 1989, ApJ, 343, 617
Djorgovski, S. B. 1985, Ph.D. thesis, Univ. of California, Berkeley
Fabbiano, G. 1989, ARA&A, 27, 87
Jedrzejewski, R. I., Davies, R. L., & Illingworth, G. D. 1987, AJ, 94, 1508
Kent, S. M. 1985, ApJS, 59, 115
Kent, S. M. 1990, in Evolution of the Universe of Galaxies, ed. R. G. Kron (ASP Conf. Ser., 10), 109
Kim, D. W. 1989, ApJ, 346, 653
Kim, D. W., Guhathakurta, P., van Gorkom, J. H., Jura, M., & Knapp, G. R. 1988, ApJ, 330, 684
Lees, J. F. 1992, ApJ, submitted
Peletier, R. F., Davies, R. L., Illingworth, G. D., Davies, L. E., & Cawson, M. 1990, AJ, 100, 1091
Persic, M., & Salucci, P. 1990, MNRAS, 245, 577
Persic, M., & Salucci, P. 1991, ApJ, 368, 60
Pizzella, A. 1989, Laurea degree thesis, "La Sapienza," Univ. of Rome
Saglia, R. P., et al. 1993, ApJ, 403, 567
Salucci, P., & Frenk, C. S. 1989, MNRAS, 237, 247
Schweizer, F., van Gorkom, J. H., & Seitzer, P. 1989, ApJ, 338, 770
Sparks, W. B., et al. 1985, MNRAS, 217, 87
van der Marel, R. P. 1991, MNRAS, 253, 710
van Gorkom, J. H., Knapp, G. R., Raimond, E., Faber, S. M., & Gallagher, J. S. 1986, AJ, 91, 791
van Gorkom, J. H., van der Hulst, J. M., Haschick, A. D., & Tubbs, A. D. 1990, AJ, 99, 1781
Varnas, S. R., Bertola, F., Galletta, G., Freeman, K. C., & Carter, D. 1987, ApJ, 313, 69